Supporting Information

Ultrafine Pt Nanoparticles Stabilized by MoS_2 / N-doped Graphene as Durable Electrocatalyst for Alcohol Oxidation and Oxygen Reduction Reactions

S. Ramakrishnan[a], Mohanraju Karuppannan[b], Mohanraj Vinothkannan[c], K. Ramachandran[a], Oh Joong Kwon[b], Dong Jin Yoo[a, c,*]

[a]R&D Education center for whole life cycle R&D of fuel cell systems, Chonbuk National University, Jeollabuk-do 54896, Republic of Korea

[b]Department of Energy and Chemical Engineering, Incheon National University, 119 Academy-ro, Yeonsu-Gu, Incheon 22012, Republic of Korea

[c]Department of Life Science, Graduate School of Department of Energy Storage/Conversion Engineering, and Hydrogen and Fuel Cell Research Center, Chonbuk National University, Jeollabuk-do 54896, Republic of Korea

---

**Corresponding authors:*

Email address: djyoo@jbnu.ac.kr (Prof. Dong Jin Yoo);

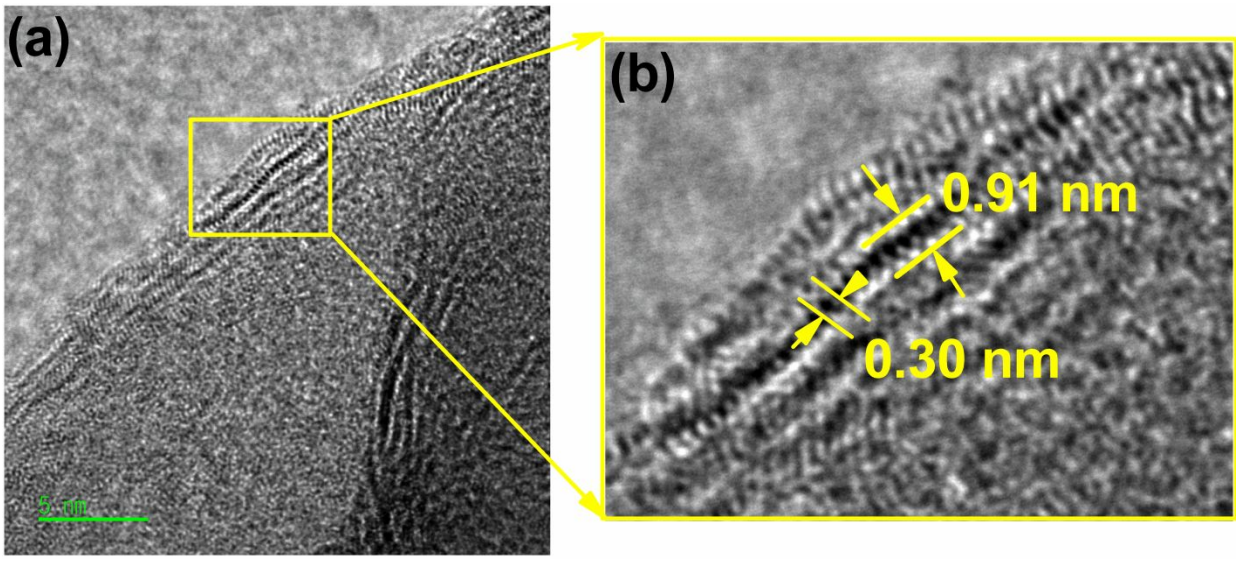

Figure S1. (a-b) HRTEM image and d-space value of MoS_2/NrGO.

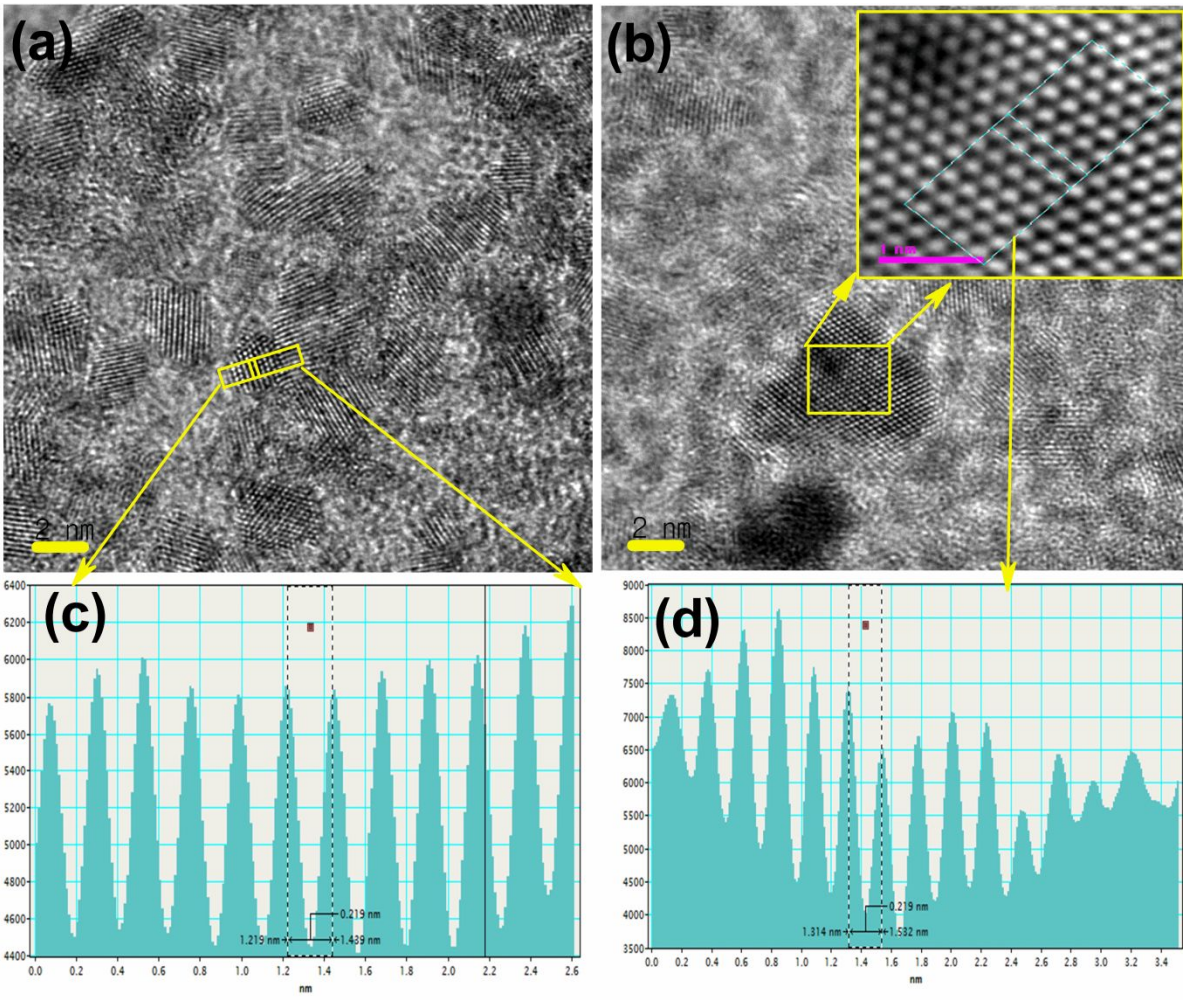

Figure S2. (a-b) HR TEM images and (c-d) d-space line profile for Pt@MoS_2/NrGO.

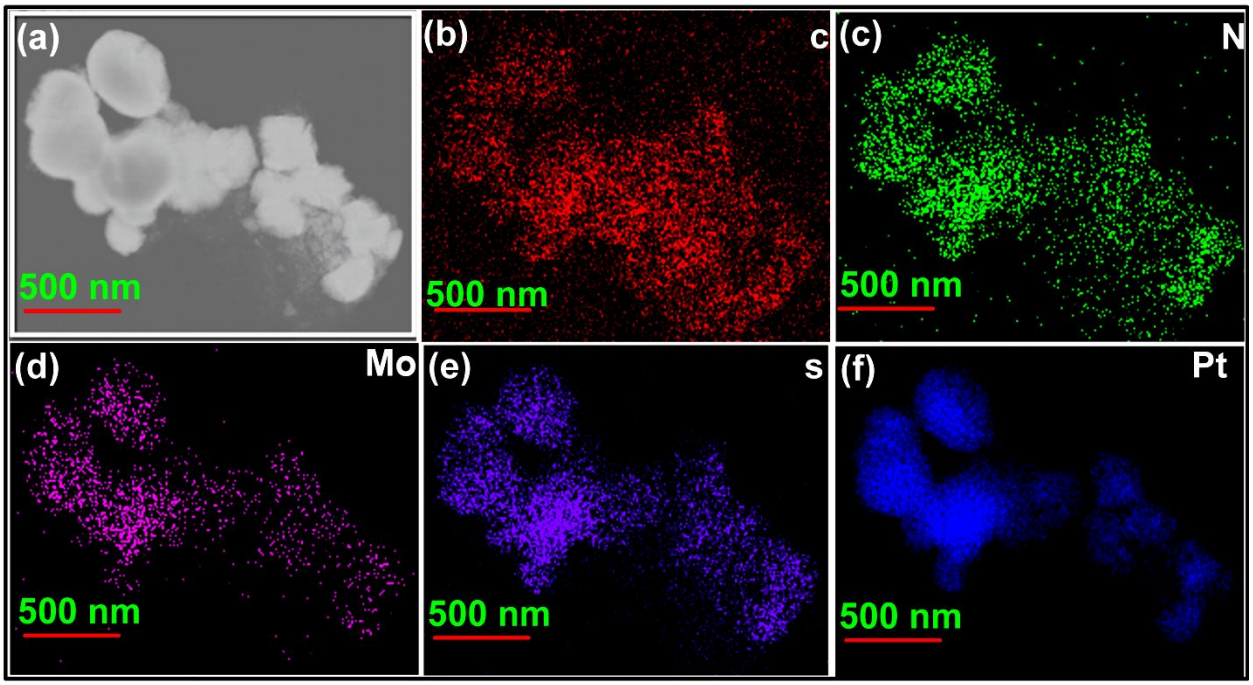

Figure S3. HAADF-STEM images of (a) Pt@MoS_2/NrGO and (b–f) the corresponding elemental mapping images.

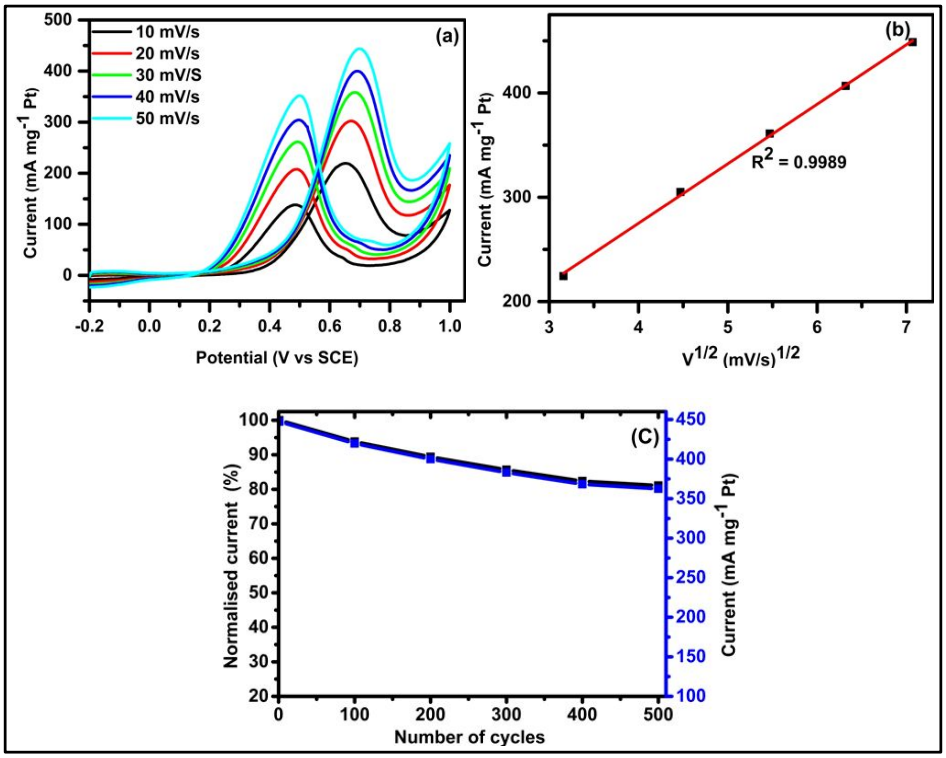

Figure S4. (a) CV curves of Pt@MoS_2/NrGO as a function of different scan rate recorded in 1 M methanol and 0.5 M H_2SO_4, (b) calibration plot of peak current density Vs square scan rate (c) Normalized current degradation as a function of cycles recorded in 1 M methanol and 0.5 M H_2SO_4.

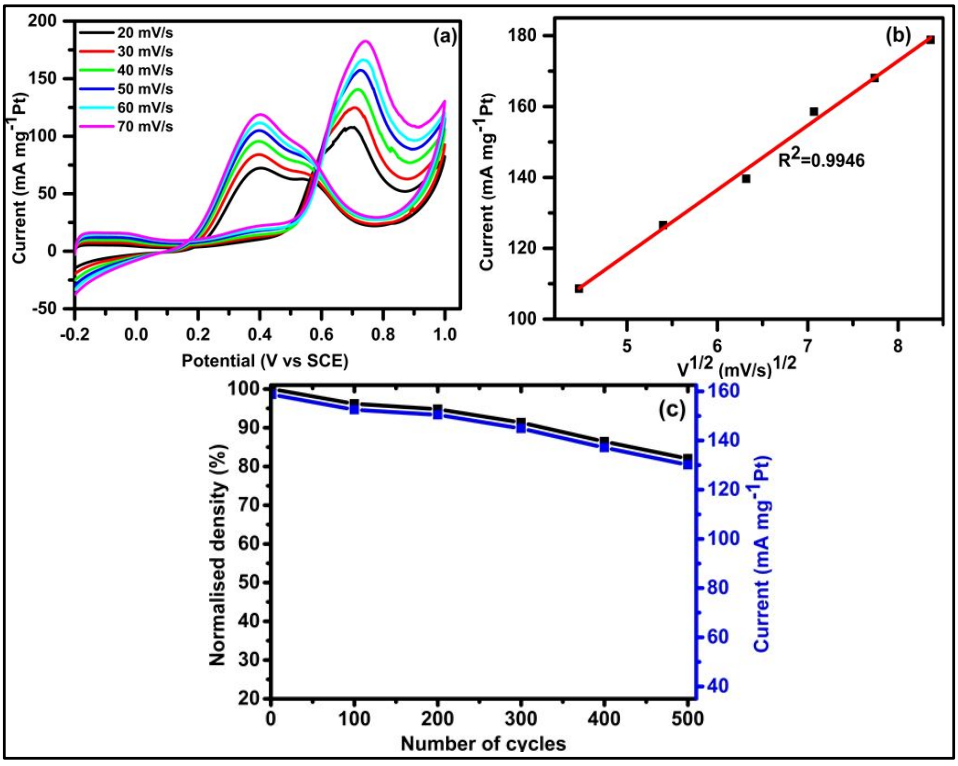

Figure S5. (a) CV curves of Pt@MoS_2/NrGO as a function of different scan rate recorded in 1 M ethylene glycol and 0.5 M H_2SO_4, (b) calibration plot of peak current density Vs square scan rate (c) Normalized current degradation as a function of cycles recorded in 1 M ethylene glycol and 0.5 M H_2SO_4.

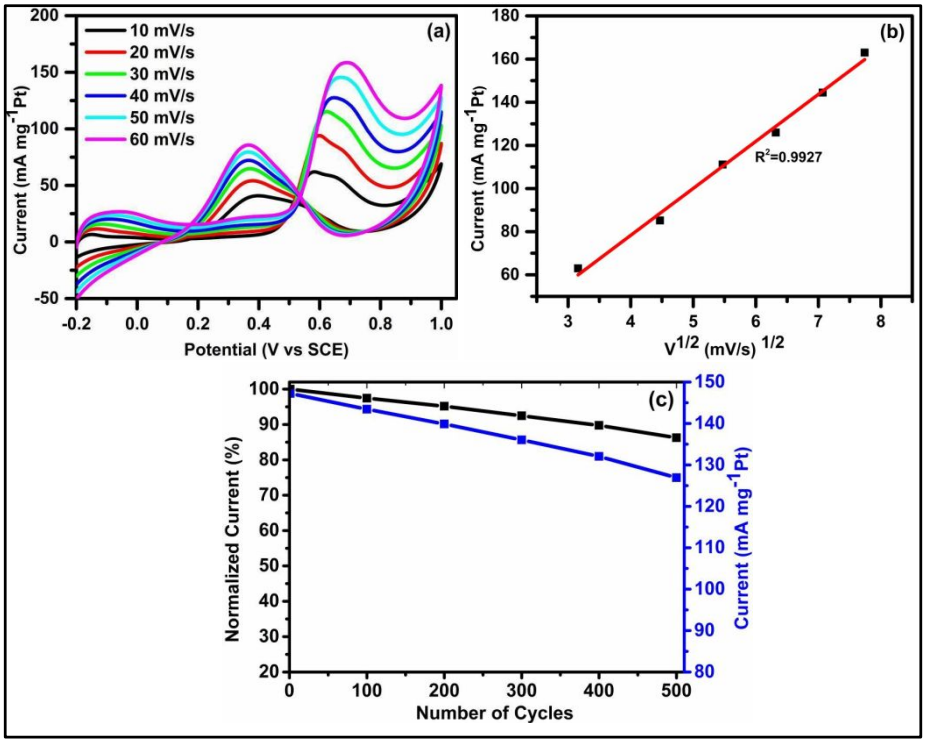

Figure S6. (a) CV curves of Pt@MoS_2/NrGO as a function of different scan rate recorded in 1 M glycerol and 0.5 M H_2SO_4, (b) calibration plot of peak current density Vs square scan rate (c) Normalized current degradation as a function of cycles recorded in 1 M glycerol and 0.5 M H_2SO_4.

The Figure S4-S6(a-b) shows the plot between current density and square root of scan rates ($V^{1/2}$) of electro-oxidation of methanol, Ethylene glycol and glycerol using Pt@MoS_2/NrGO catalyst and its fitting sows good liner relationship with R^2 values are 0.9989, 0.9946 & 0.9927 corresponding to electro oxidation methanol, ethylene glycol and glycerol respectively. The

results are illustrates the alcohols oxidation reaction on Pt@MoS_2/NrGO electrode is diffusion controlled process.

Table S1. Comparisons of exiting electrocatalysts for alcohol oxidation.

Electrode Materials	Fuel		Electrolyte		Current density (mA mg^{-1}_{Pt})	Reference
	Type	Concentration (M)	Type	Concentration (M)		
Au@Pt/MoS_2	Methanol	1	KOH	0.5	6240	[1]
Pd–MoS_2	Methanol	1	KOH	0.5	433.5	[2]
Pt-MoS_2/N doped bio carbon	Methanol	0.5	H_2SO_4	0.5	1030.2	[3]
Pt-Ce_{2-x}/GNS	Methanol	1	KOH	1	1159	[4]
	Ethylene Glycol	1	KOH	1	3260	
	Glycerol	1	KOH	1	2550	
PdPb alloy nanotubes	Ethylene glycol	1	KOH	1	4060	[5]
	Glycerol	1	KOH	1	2220	
PdAu/NG	Ethylene glycol	1	KOH	1	12800	[6]
	Glycerol	1	KOH	1	8700	
graphene–MWCNTs/Pt	Methanol	1	H_2SO_4	0.5	168.41	[7]
	Ethylene glycerol	1	H2SO4	0.5	153.13	
Pd/RGO	Ethylene glycerol	0.5	KOH	0.5	33.7	[8]
	Glycerol	0.5	KOH	0.5	25.1	
Pt@MoS_2/NrGO	Methanol	1	H_2SO_4	0.5	448	Present work
	Ethylene glycol	1	H_2SO_4	0.5	158	
	Glycerol	1	H_2SO_4	0.5	147	

Koutecky–Levich (K–L) plots

Using Equation (1) Koutecky–Levich (K–L) plots are derived from plots of inverse of current density (i_d^{-1}) and inverse of the square root of the rotation rate ($\omega^{-1/2}$)

$$I_K = \frac{I_d I}{I_d - I} \qquad (1)$$

Where I is experimentally measured current density

I_K is Kinetic current density

I_d *is* Diffusion limited current density

Number of electron calculation

$0.62nFAD^{2/3}Cv^{-1/6}\omega^{1/2}$ (2)

A is Geometric area of electrode (0.19625 cm-2

C -is bulk O_2 solubility of 1.18×10^{-6} mol cm^{-3}

D_{O2} is diffusion co-efficient of oxygen of $1.9 \times 10^{-5} cm^2 s^{-1}$

V is Kinetic viscosity of 8.93×10^{-3} $cm^2 s^{-1}$ in 0.1 M $HClO_4$

n is number of electron transfer per oxygen molecular during the ORR

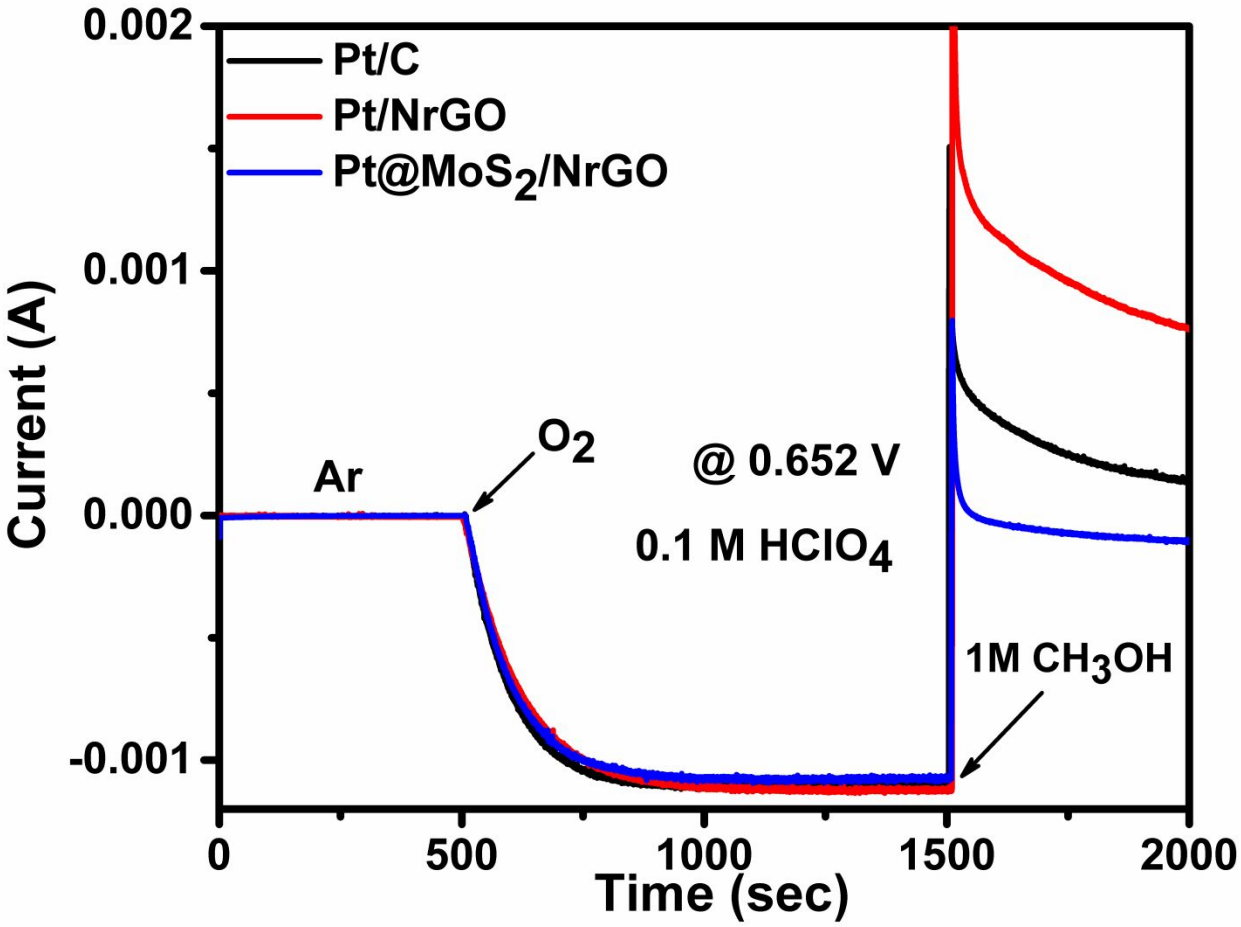

Figure S7. Chronoamperometry response of $Pt@MoS_2$/NrGO, Pt@NrGO and Pt/C electrode in presence of Ar / O_2 / O_2 + 1 M CH_3OH in 0.1 M $HClO_4$ at 1600 rpm.

Furthermore, the methanol tolerance study was also performed for $Pt@MoS_2$/NrGO, Pt@NrGO and Pt/C electrodes using chronoamperometry techniques. The modified electrodes were polarized with fixed potential of 0.652 V vs RHE upto 2000 s with rotation of 1600 rpm in 0.1 M $HClO_4$. The electrolyte was purged with argon upto 500 seconds and oxygen purged from 500 to 2000 seconds and then methanol introduced at 1500 seconds. In Figure S7, $Pt@MoS_2$/NrGO, Pt@NrGO and Pt/C electrodes shows almost similar oxygen reduction response from 500 to 1500 s, but once introduce the methanol at 1500 s, the ORR activity was significantly distrubed. It is identified that $Pt@MoS_2$/NrGO electrode has less disturbance than others and shows reduction current at 2000 s. This study reveals that $Pt@MoS_2$/NrGO has low methanol tolerance properties, even though it is better than commercial Pt/C and Pt/NrGO electrocatalysts.

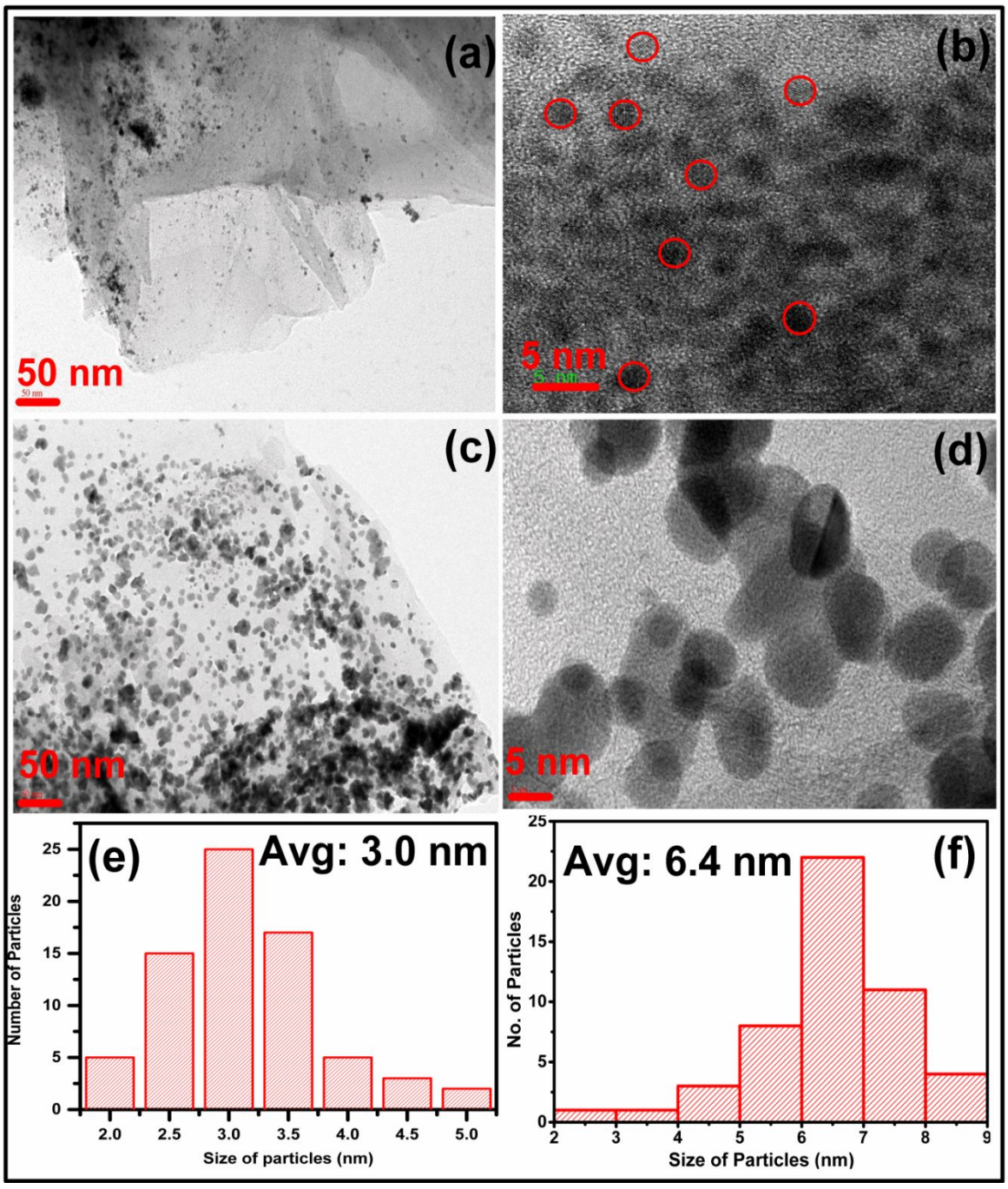

Figure S8. TEM images of Pt@MoS_2/NrGO (a and b) taken before 30000 potential cycles and (c and d) taken after 30000 potential cycles; corresponding particle size histograms of (e) before 30000 potential cycles and (f) after 30000 potential cycles.

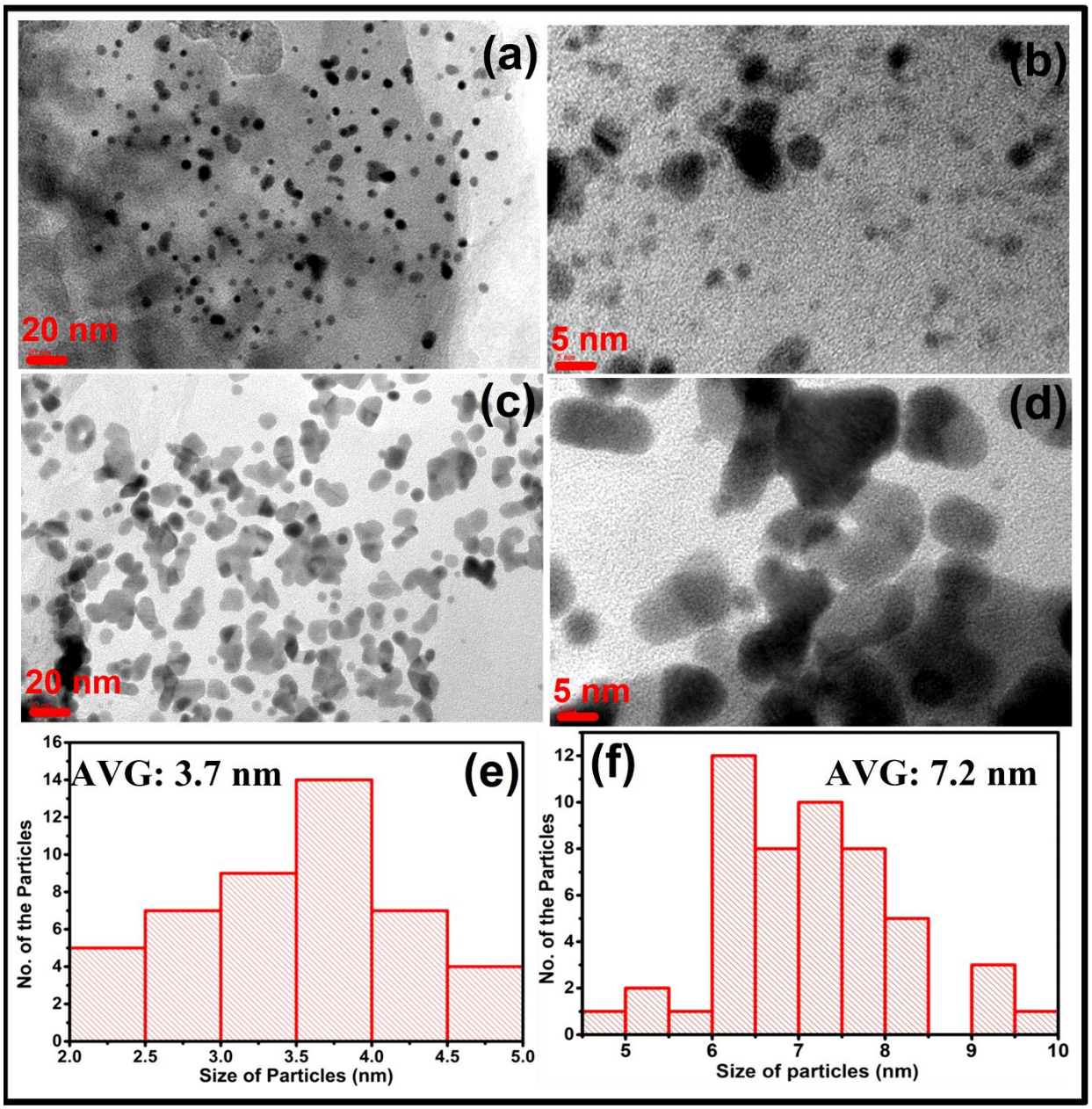

Figure S9. TEM images of Pt@NrGO (a and b) taken before 30000 potential cycles and (c and d) taken after 30000 potential cycles; corresponding particle size histograms of (e) before 30000 potential cycles and (f) after 30000 potential cycles.

References

S1. Su, S.; Zhang, C.; Yuwen, L.; Liu, X.; Wang, L.; Fan, C.; Wang, L., Uniform Au@Pt core–shell nanodendrites supported on molybdenum disulfide nanosheets for the methanol oxidation reaction. *Nanoscale* **2016,** *8* (1), 602-608.

S2. Yuwen, L.; Xu, F.; Xue, B.; Luo, Z.; Zhang, Q.; Bao, B.; Su, S.; Weng, L.; Huang, W.; Wang, L., General synthesis of noble metal (Au, Ag, Pd, Pt) nanocrystal modified MoS2 nanosheets and the enhanced catalytic activity of Pd–MoS2 for methanol oxidation. *Nanoscale* **2014,** *6* (11), 5762-5769.

S3. Tang, B.; Lin, Y.; Xing, Z.; Duan, Y.; Pan, S.; Dai, Y.; Yu, J.; Zou, J., Porous coral reefs-like MoS2/nitrogen-doped bio-carbon as an excellent Pt support/co-catalyst with promising catalytic activity and CO-tolerance for methanol oxidation reaction. Acta .Electrochim **2017,** *246*, 517-527.

S4. He, Q.; Shen, Y.; Xiao, K.; Xi, J.; Qiu, X., Alcohol electro-oxidation on platinum–ceria/graphene nanosheet in alkaline solutions. *Int. J. Hydrog. Energy* **2016,** *41* (45), 20709-20719.

S5. Xu, H.; Song, P.; Fernandez, C.; Wang, J.; Zhu, M.; Shiraishi, Y.; Du, Y., Sophisticated Construction of Binary PdPb Alloy Nanocubes as Robust Electrocatalysts toward Ethylene Glycol and Glycerol Oxidation. *ACS Appl. Mater. Interfaces* **2018,** *10* (15), 12659-12665.

S6. Zhai, C.; Hu, J.; Zeng, L.; Fu, N.; Du, Y.; Zhu, M., One-pot fabrication of Nitrogen-doped graphene supported binary palladium-sliver nanocapsules enable efficient ethylene glycol electrocatalysis. *J. Colloid Interface Sci.* **2019,** *535*, 392-399.

S7. Gorle, D. B.; Kulandainathan, M. A., One-pot synthesis of highly efficient graphene based three-dimensional hybrids as catalyst supporting materials for electro-oxidation of liquid fuels. *J. Mater. Chem. A* **2017,** *5* (29), 15273-15286.

S8. Li, S.-S.; Hu, Y.-Y.; Feng, J.-J.; Lv, Z.-Y.; Chen, J.-R.; Wang, A.-J., Rapid room-temperature synthesis of Pd nanodendrites on reduced graphene oxide for catalytic oxidation of ethylene glycol and glycerol. *Int. J. Hydrog. Energy* **2014,** *39* (8), 3730-3738.